Stochastic Geometry-based Analysis of Joint Radar and Communication-Enabled Cooperative Detection Systems

Dorsaf Ghozlani [12], Aymen Omri [1], Seifeddine Bouallegue [3], Hela Chamkhia [1], Ridha Bouallegue [1].
[1]Innovation of Communicant & Cooperative Mobiles (Innov'Com) Lab (SUP'COM)
Higher School of Communications of Tunis, University of Carthage, Ariana, Tunisia
[2]National Engineering School of Tunis, University of Tunis El Manar, Tunis, Tunisia.
[3]College of the North Atlantic, Doha, Qatar.
Email: {dorsaf.ghozlani, aymen.omri, hela.chamkhia, ridha.bouallegue}@supcom.tn.
and seifeddine.bouallegue@cna-qatar.edu.qa.

***Abstract*—Traditionally, the communication and radar are separately designed. Recently, and with 5G technology, the Millimeter Wave (mmWave) spectrum becomes paramount for the exploitation of the large bandwidths. However, the interference problems have negative impacts on both radar and communication systems. To overcome these problems, the joint radar and communication (JRC) systems has been proposed as a promising technique that improves the spectrum utilization, allowing an optimal spectrum sharing and an efficient cooperative detection.**

In this paper, we propose an accurate performance analysis of JRC-enabled cooperative detection systems, where stochastic geometry is used to model the different vehicle positions in a given JRC systems. We derive closed form expressions of the average cooperative detection range (CDR) for different scenarios, with a different number of vehicles. Based on that, the general average CDR expression for a general number of vehicles has been derived. The results confirm the derived analytical expressions, which present efficient metrics to evaluate the cooperative detection in JRC systems.

***Index Terms*—Joint Radar Communication, Cooperative Detection Range, Stochastic Geometry.**

I. Introduction

In recent years, vehicle-to-vehicle (V2V) communications have received an increasing attention as a promising concept. It can offer a low latency of message transfer when compared to interchange raw sensor data [1]. However, with the increasing number of vehicles, using below 6 GHz carrier frequencies becomes difficult for some communication types, such as the IEEE 802.11ad with a 2.16 GHz of bandwidth, and which is based on the Dedicated Short-Range Communication (DSRC) [2], [3]. In fact, DSRC achieves data rates of at most 27 Mbps, which does not meet application requirements, such as fully automated driving and adaptive cruise control. Moreover, it doesn't maintain the gigabit-per-second data rates that is necessary for raw sensor data exchange between vehicles [4]. Consequently, automotive communication systems have switched to millimeter-wave band to overcome exploiting small band problems.

While the communication takes advantage of the large bandwidths available in the mmWave spectrum [5], interference in both radar and communication systems can not be neglected. Moreover, there is a limitation of the millimeter-wave automotive radar to detect surroundings which will demand very high system performance and operation by increasing signal directionality and power [6]. The JRC has attracted substantial attention not only for improving the spectrum utilization but also for achieve high-speed signal processing and information integration.

Recently, various research attempts have been focusing on exploiting the same device and radio spectrum for joint radar-communication [7], [8]. By taking the advantage of spectrum sharing, the JRC allows communication systems and individual radar to share spectrum bands and hence, improves the spectrum utilization. JRC is able to enhance the performance and the efficiency of resources, such as reducing the system size, and minimizing the system cost. This is due to the fact that JRC allows an autonomous vehicle, and a single hardware platform to simultaneously perform the communication function and the radar function [9], [10]. Accordingly, sharing the spectrum bands becomes an important issue.

The 77 GHz millimeter-wave band can be used by the radar devices installed on autonomous vehicles [11]. The method of spectrum sharing improves the performance of the cooperative system [12], [13]. However the communication system uses a separate part of the radar spectrum band. Using one radar, this separation can degrade the performance of the system [14]. Nevertheless, using cooperative detection, can improve the performance of radar compared to single detection mode [15].

In the literature, few research works have been focusing on JRC-enabled cooperative detection systems. In [16], the authors have proposed a joint target detection system based on multiple cooperative radar mode-enabled base stations (BSs). Based on that, they have evaluated the impact of BS cooperation on the detection performance of mmWave

978-1-6654-2854-5/21/$31.00 ©2021 IEEE

RadCom systems. In another work, stochastic geometry has been used in [17] to analyze the performance of JRC enabled cooperative detection for drone surveillance, where the surveillance drone radars are designed to detect targets with the main beams, then share the detection information with the corresponding sub beams. Accordingly, the authors have defined the concept of the detection volume which is the union of the cooperative detection regions [17]. Then, they have derived the corresponding expression to evaluate the performance of the considered JRC-enabled cooperative detection system. In the same context, the average cooperative detection area for JRC-enabled cooperative unmanned aerial vehicle (UAV) network has been studied in [18], where the upper bound expression of the corresponding cooperative detection area has been derived. In this paper, and different from the aforementioned work in the literature, we propose a new performance analysis of JRC-enabled cooperative detection systems. Stochastic geometry is used to model the different vehicle positions in a given JRC systems. Based on that, we consider three scenarios that are defined by different number of vehicles. For each scenario, we detail and derive the closed form expression of the average cooperative detection range (CDR). The general average CDR expression for a general number of vehicles has been derived. The remainder of this paper is organized as follows: Section II describes the system model and its analytical expressions. Section III details the performance analysis. In Section IV, the simulation steps and the numerical results are presented, where the accuracy of the derived expressions and the relevant analysis are highlighted. Finally, conclusions are drawn in Section V.

II. System Model

In this section, we describe the system model of a JRC systems in a 1-D space. The system model consists of vehicles arranged according to Poisson Point Process (PPP) Φ, with density λ. A single vehicle is not able to detect targets that are outwardly far of self-detection range. The cooperation between vehicles using JRC is a solution to enhance detection range and assist vehicles to make rapid decision to avoid collision.

We denote by r, the distance in meters, between each two vehicles. Let R_r and R_c be the radius of radar detection range and communication detection range, respectively.

By assuming that the communication range R_c is greater than radius R_r of radar range, each vehicle, communicates with the nearest vehicle.

We consider that the nearest vehicle is located at a distance r from the transmitting vehicle. For a given distance R, the probability $P\{R > r\}$ is expressed by one minus the null probability of a 1-D PPP where vehicle is located in the 1-D space, and its expression is given by [19].

$$\begin{aligned} P\{R > r\} &= 1 - P\{R < r\} \\ &= 1 - \exp(-\lambda R). \end{aligned} \tag{1}$$

Based on (1), and by using the expression of the complementary cumulative distribution function (CCDF) [20], the PDF of r can be approximated as follows [21]:

$$f(r) \approx \lambda \exp(-\lambda r). \tag{2}$$

We denote by B the radar spectrum band. To coordinate between radar and communication detection range, and to share spectrum band, we consider $B_c = \eta B$, and $B_r = (1-\eta)B$, are the bandwidth of communication and radar, respectively, where η is a coefficient that determines the separation of both radar and communication parts.
In the next section, we will study and detail the cooperative detection range of JRC systems, in different scenarios.

III. Performance Analysis of the Cooperative Detection Range

In this section, we analyse the performance of a general JRC systems in terms of the cooperative detection range. We derive the corresponding expression that is based mainly on the number of vehicles and the distances between each two adjacent vehicles.
Accordingly, in this work, we consider the following three scenarios

A. Scenario I :Two vehicles

In this scenario, there are two different cases as shown in Fig. 1.

- Case 1: In this case, the radar detection regions are overlapping, and the overlapping distance $L_{overlap} = 2R_r - r$, where the distance r between the two vehicles is less than $2R_r$. Accordingly, the $CDR = 4R_r - L_{overlap}$.
- Case 2: In this case, there is no overlap radar ranges, where $2R_r < r \leq R_c$, and the $CDR = 4R_r$.

Consequently, the average CDR of senario I, can be written as follows:

$$\begin{aligned} \overline{CDR}_I &= \int_0^{2R_r} (2R_r + r) f(r)\ dr + \int_{2R_r}^{R_c} 4R_r f(r)\ dr \\ &= \int_0^{2R_r} 2R_r \lambda \exp(-\lambda r) + r\lambda \exp(-\lambda r) dr \\ &\quad + \int_{2R_r}^{R_c} 4R_r \lambda \exp(-\lambda r) dr. \end{aligned} \tag{3}$$

By using the expression of f in (2), the integrations in (3) are evaluated, and the final $\overline{CDR}$ expression is given by

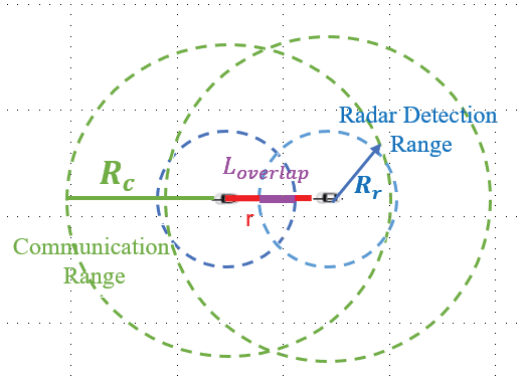

(a) Case 1.

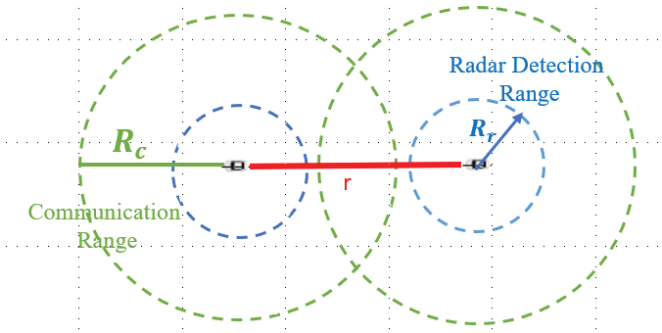

(b) Case 2.

Fig. 1: Scenario I

$$\overline{CDR}_I = 2R_r + 2\Big[-\exp(-\lambda R_c) + \exp(-2\lambda R_r)\Big]R_r + \frac{1-\exp(-2\lambda R_r)(1+2\lambda R_r)}{\lambda}. \quad (4)$$

B. Scenario II :Three vehicles

Let r_1 and r_2 are the distances between the vehicles 1 and 2, and the vehicles 2 and 3, respectively. Based on the values of these distances, we have the following four cases, in this scenarios:

- Case 1: As shown in Fig. 2, in this case, the radar detection regions of vehicles 1 and 2 are overlapping, when $r_1 < 2R_r$, and hence $CDR = 6R_r - L_{1overlap}$.
- Case 2: In this case, the radar detection regions of vehicles 2 and 3 are overlapping, when $r_2 < 2R_r$, and hence the CDR expression is equal to $6R_r - L_{2overlap}$.
- Case 3: In this case, the radar detection ranges of all the adjacent vehicles are overlapping, where both distances are less than $2R_r$ as presented in Fig. 2. Consequently, $CDR = 6R_r - L_{1overlap} - L_{2overlap}$.
- Case 4: No overlapping can be observed in this case, when $2R_r < r_1 \leq R_c$ and $2R_r < r_2 \leq R_c$. Accordingly, CDR =$6R_r$.

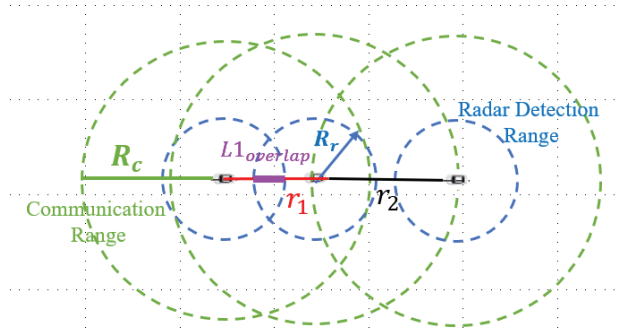

(a) Case 1.

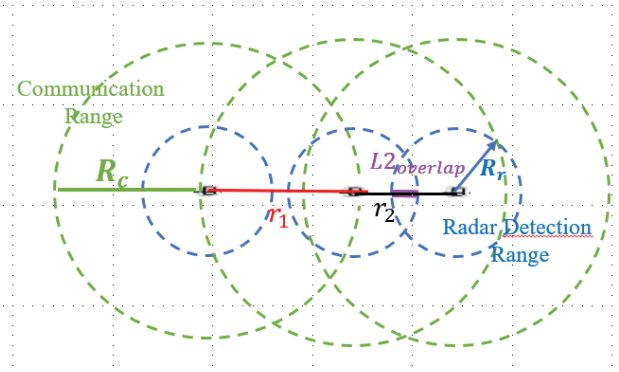

(b) Case 2.

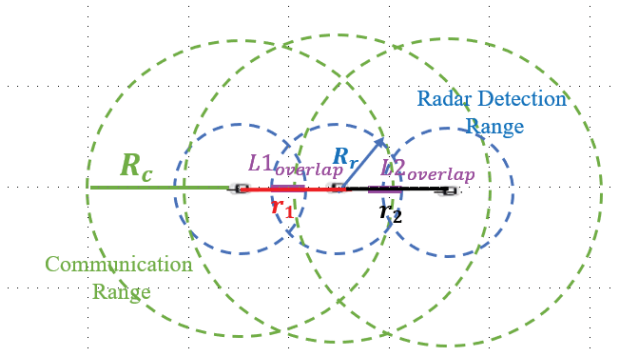

(c) Case 3.

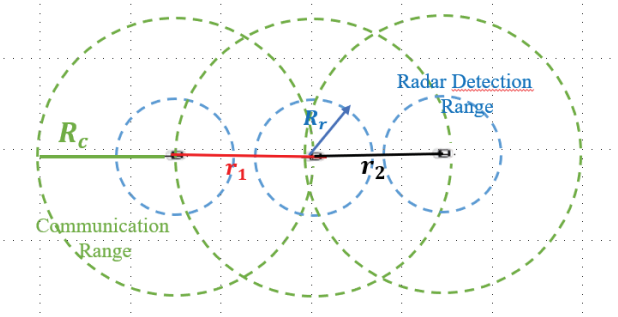

(d) Case 4.

Fig. 2: Scenario II

Based on that, the corresponding average CDR expression can be rewritten as follows:

$$\overline{CDR}_{II} = 2\int_0^{2R_r}\Big(4R_r\lambda\exp(-\lambda r_1)+r_1\lambda\exp(-\lambda r_1)\Big)dr_1 \times\int_{2R_r}^{R_c}\lambda\exp(-\lambda r_2)dr_2+\Big[\int_0^{2R_r}2R_r\lambda\exp(-\lambda r_1)dr_1 +\int_0^{2R_r}\Big(2r_1\lambda\exp(-\lambda r_1)\Big)dr_1\Big]\int_0^{2R_r}\Big(\lambda\exp(-\lambda r_2)\Big)dr_2 +\int_{2R_r}^{R_c}\Big(6R_r\Big(\lambda\exp(-\lambda r_1)\Big)dr_1\Big)\int_{2R_r}^{R_c}\lambda\exp(-\lambda r_2)dr_2 \quad (5)$$

After evaluating the integrals in (5), and making some simplification the final expression of $\overline{CDR}_{II}$ is given by:

$$\overline{CDR}_{II} = \Big[2R_r+4\Big(-2\exp(-\lambda R_c)-\exp(-2\lambda R_r)\Big)R_r +2\Big(\frac{1-\exp(-2\lambda R_r)\Big(1+2\lambda R_r\Big)}{\lambda}\Big)\Big]\Big(1-\exp(-\lambda R_c)\Big) +\Big[6R_r\exp(-\lambda R_c)-4R_r\exp(-2\lambda R_r)\Big]\Big(\exp(-\lambda R_c)\Big). \quad (6)$$

C. Scenario III :Four vehicles

In this case, we have four vehicles, where r_1 ,r_2, and r_3 are the corresponding inter-distances between the adjacent vehicles. Accordingly, we have the following 8 cases:

- Case 1:
if ($r_1 < 2R_r$ & $r_2 < 2R_r$ & $r_3 < 2R_r$) **then**
CDR= $8R_r - (L_{1overlap} + L_{2overlap} + L_{3overlap})$.

- Case 2:
if ($r_1 < 2R_r$ & $r_2 < 2R_r$ & $2R_r < r_1 \leq R_c$) **then**
CDR= $8R_r - (L_{1overlap} + L_{2overlap})$.

- Case 3:
if ($2R_r < r_1 \leq R_c$ & $r_2 < 2R_r$ & $r_3 < 2R_r$) **then**
CDR= $8R_r - (L_{2overlap} + L_{3overlap})$.

- Case 4:
if ($r_1 < 2R_r$ & $2R_r < r_2 \leq R_c$ & $r_3 < 2R_r$) **then**
CDR= $8R_r - (L_{1overlap} + L_{3overlap})$.

- Case 5:
if ($r_1 < 2R_r$ & $2R_r < r_2 \leq R_c$ & $2R_r < r_3 \leq R_c$) **then**
CDR= $8R_r - L_{1overlap}$.

- Case 6:
if ($2R_r < r_1 \leq R_c$ & $r_2 < 2R_r$ & $2R_r < r_3 \leq R_c$) **then**
CDR= $8R_r - L_{2overlap}$.

- Case 7:
if ($2R_r < r_1 \leq R_c$ & $2R_r < r_2 \leq R_c$ & $r_3 < 2R_r$) **then**
CDR= $8R_r - L_{3overlap}$.

- Case 8:
if ($2R_r < r_1 \leq R_c$ & $2R_r < r_2 \leq R_c$ & $2R_r < r_3 \leq R_c$) **then**
CDR= $8R_r$.

Based on the presented 8 cases, we have derived the average CDR of this scenario, by following the same presented derivation details for scenarios 1 and 2, which yields to the final expression that is presented in (7).

D. General formula

Based on the previous derived average CDR expressions, we present in this section, the general expression for a general number of considered vehicles.
Let n be a given number of considered vehicles, and I be the corresponding number of overlapping radar detection regions. By evaluating the values of I, we have identified a relationship between the I values and the number n. This relationship is presented in Table I for examples of $n = 2,\ ,3,\ 4$ and 5, where

$$A = \Big(-\exp(-\lambda R_c)+\exp(-2\lambda R_r)\Big), \quad (8)$$

$$B = \Big(\frac{1-\exp(-2\lambda R_r)(1+2\lambda R_r)}{\lambda}\Big), \quad (9)$$

$$C = \Big(1-\exp(-2\lambda R_r)\Big), \quad (10)$$

and,

$$D = \exp(-2\lambda R_r). \quad (11)$$

For each value of I, and based on the previous derived expressions, we have derived the corresponding CDR expressions. Finally, we have gathered all the possible values of I for a given number of vehicles n weighted by the corresponding expression of CDR to get the following final expression of the average CDR.

$$\overline{CDR}(n) = \sum_{I=0}^{n-1}\Bigg[\delta(I)\ 2nR_rA^{n-1} +\frac{(n-I)\times(n-I+1)\times(n-I+2)\times\ldots(n-1)}{I!} \times\Big\lceil\frac{I}{I+1}\Big\rceil\Big(2(n-I)R_r-2(n-I)R_rD+I\ B\Big) \times C^{I-1}A^{n-I-1}\Bigg], \quad (12)$$

where,

$$\delta(I) = 2nR_r\Big(-\exp(-\lambda R_c)+\exp(-2\lambda R_r)\Big)^{n-1} \quad (13)$$

IV. Numerical Results

In this section, we present the numerical results to evaluate the derived average CDR expressions of the different scenarios.

A. Simulation Setup

We consider a 1-D space region, where many vehicles are located in a road of length $R = 1000$ m. The vehicles are distribute daccording to a Poisson point process PPP, with different values of λ, R_c, and R_r.

$$\overline{CDR}_{III} = \Big[18R_r + 2\Big(- 5\exp(-2\lambda R_r) - 4\exp(-\lambda R_c)\Big)R_r + 3\Big(\frac{1-\exp(-2\lambda R_r)\Big(1+2\lambda R_r\Big)}{\lambda}\Big)\Big]$$
$$\times\Big(- \exp(-\lambda R_c) + \exp(-2\lambda R_r)\Big)^2 + 3\Big[4R_r - 4R_r\exp(-2\lambda R_r) + 2\Big(\frac{1-\exp(-2\lambda R_r)\Big(1+2\lambda R_r\Big)}{\lambda}\Big)\Big]\Big(1-\exp(-2\lambda R_r)\Big)$$
$$\times\Big(- \exp(-\lambda R_c) + \exp(-2\lambda R_r)\Big) + \Big[2R_r - 2R_r\exp(-2\lambda R_r) + 3\Big(\frac{1-\exp(-2\lambda R_r)\Big(1+2\lambda R_r\Big)}{\lambda}\Big)\Big]\Big(1-\exp(-2\lambda R_r)\Big)^2. \quad (7)$$

TABLE I: Relationchip between the number of vehicule n and the corresponding number of overlapping radar detection regions I, for $n = 2,\ 3,\ 4$, and 5

n	I=0	I=1	I=2	I=3	I=4
2	$1[4\ R_r A]$	$1[2R_r - 2R_r D + B]$			
3	$1[6\ R_r A^2]$	$2[4R_r - 4R_r D + B]\ A$	$1[2R_r - 2R_r D + 2B]\ C$		
4	$1[8\ R_r A^3]$	$3[6R_r - 6R_r D + B]\ A^2$	$3[4R_r - 4R_r D + 2B]\ CA$	$1[2R_r - 2R_r D + 3B]\ C^2$	
5	$1[10\ R_r A^4]$	$4[8R_r - 8R_r D + B]\ A^3$	$6[6R_r - 6R_r D + 2B]\ CA^2$	$4[4R_r - 4R_r D + 3B]\ C^2 A$	$1[2R_r - 2R_r D + 4B]\ C^2$

B. Simulation Results Interpretation

Fig. 3 presents the variations of the average CDR versus R_c, with $\lambda = 0.1$ m^{-1}, and $R_r = 0.3\ R_c$. As shown in this figure, by increasing the values of communication range R_c, the average CDR increases. This is due to the fact that with the increase of R_c, the probability of a possible cooperation increases. In addition, it is clear that the CDR increases with the increased number of vehicles, which is expected. Also, the simulation results confirm the accuracy of our expression derivations for the different scenarios.

Fig. 4 shows the average CDR versus R_r. Similar to the behavior of the CDR variation vs. R_c that is presented in Fig. 3, the average CDR increases with the increased values of R_r. This is because the total coverage range is related to R_r, and hence, by increasing R_r, a significant enhancement of the CDR can be observed for the different scenarios.

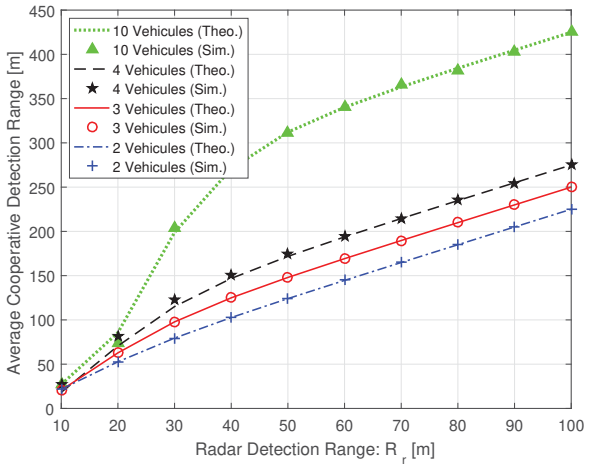

Fig. 4: Average cooperative detection range vs. R_r

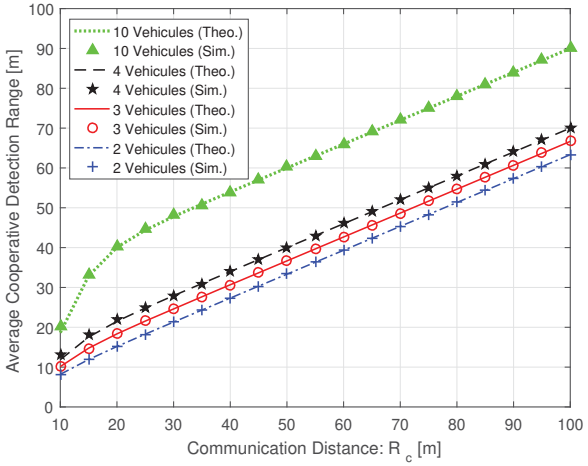

Fig. 3: Average cooperative detection range vs. R_c

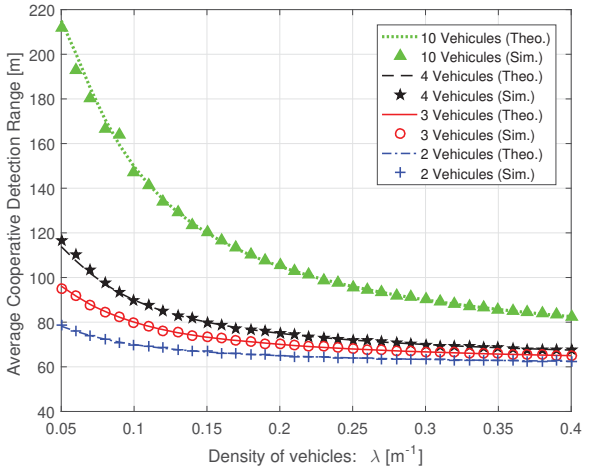

Fig. 5: Average cooperative detection range vs. λ

Fig. 5 presents the average CDR versus λ. It is clear that the average CDR decreases with the increased values of λ. This is because, by increasing the values of λ, the number of vehicles increases too, where they become closer to each other. Consequently, the distances between the vehicles decrease to be lower than $2R_r$. Thus, several areas of overlap occur which decreases the average CDR.

V. Conclusion

In this paper, stochastic geometry-based analysis of JRC systems CDR has been presented and detailed. The average CDR expression for a given set of parameters has been derived for three scenarios of two, three, and four vehicles. For each scenario, we have detailed and derived the CDR closed form expression. Based on that, the general average CDR expression for a general number of vehicles has been derived. Simulation results have been conducted to evaluate the analytical results and investigate the different studied scenarios, where the accuracy of the general average CDR expression has been confirmed regardless of the number of vehicles.

Acknowledgement

This work was supported by the project "783119-1 SECREDAS Product Security for Cross Domain Reliable Dependable Automated System, H2020- ECSEL, EU"

References

[1] V. Jain et al., "Prediction based framework for vehicle platooning using vehicular communications," in *2017 IEEE Vehicular Networking Conference (VNC)*, 2017, pp. 159–166.

[2] Junil Choi, Vutha Va, Nuria Gonzalez-Prelcic, Robert Daniels, Chandra R Bhat, and Robert W Heath, "Millimeter-wave vehicular communication to support massive automotive sensing," *IEEE Communications Magazine*, vol. 54, no. 12, pp. 160–167, 2016.

[3] Andrea Tassi, Malcolm Egan, Robert J Piechocki, and Andrew Nix, "Modeling and design of millimeter-wave networks for highway vehicular communication," *IEEE Transactions on Vehicular Technology*, vol. 66, no. 12, pp. 10676–10691, 2017.

[4] Junil Choi, Vutha Va, Nuria Gonzalez-Prelcic, Robert Daniels, Chandra R Bhat, and Robert W Heath, "Millimeter-wave vehicular communication to support massive automotive sensing," *IEEE Communications Magazine*, vol. 54, no. 12, pp. 160–167, 2016.

[5] Soumaya Bachtobji, Aymen Omri, and Ridha Bouallegue, "Modelling and performance analysis of 3-d mmwaves based heterogeneous networks," in *2016 International Wireless Communications and Mobile Computing Conference (IWCMC)*, 2016, pp. 72–76.

[6] Hao Ma, Zhiqing Wei, Jiaxin Zhang, Fan Ning, and Zhiyong Feng, "Three-dimensional multiple access method for joint radar and communication enabled v2x network," pp. 1–5, 2019.

[7] Robert C Daniels, Enoch R Yeh, and Robert W Heath, "Forward collision vehicular radar with ieee 802.11: Feasibility demonstration through measurements," *IEEE Transactions on Vehicular Technology*, vol. 67, no. 2, pp. 1404–1416, 2017.

[8] Julien Le Kernec and Olivier Romain, "Performances of multitones for ultra-wideband software-defined radar," *IEEE Access*, vol. 5, pp. 6570–6588, 2017.

[9] Nguyen Cong Luong, Xiao Lu, Dinh Thai Hoang, Dusit Niyato, and Dong In Kim, "Radio resource management in joint radar and communication: A comprehensive survey," *arXiv preprint arXiv:2007.13146*, 2020.

[10] Kumar Vijay Mishra, MR Bhavani Shankar, Visa Koivunen, Bjorn Ottersten, and Sergiy A Vorobyov, "Toward millimeter-wave joint radar communications: A signal processing perspective," *IEEE Signal Processing Magazine*, vol. 36, no. 5, pp. 100–114, 2019.

[11] Jürgen Hasch, Eray Topak, Raik Schnabel, Thomas Zwick, Robert Weigel, and Christian Waldschmidt, "Millimeter-wave technology for automotive radar sensors in the 77 ghz frequency band," *IEEE Transactions on Microwave Theory and Techniques*, vol. 60, no. 3, pp. 845–860, 2012.

[12] Aymen Omri, Mazen O. Hasna, and Khaled B. Letaief, "Inter-relay interference management schemes for wireless multi-user decode-and-forward relay networks," *IEEE Transactions on Wireless Communications*, vol. 14, no. 4, pp. 2072–2081, 2015.

[13] Aymen Omri and Mazen O. Hasna, "Physical layer security analysis of uav based communication networks," in *2018 IEEE 88th Vehicular Technology Conference (VTC-Fall)*, 2018, pp. 1–6.

[14] Mark A Richards, Jim Scheer, William A Holm, and William L Melvin, "Principles of modern radar," 2010.

[15] Andrew Herschfelt and Daniel W Bliss, "Spectrum management and advanced receiver techniques (smart): Joint radar-communications network performance," pp. 1078–1083, 2018.

[16] C. Skouroumounis, C. Psomas, and I. Krikidis, "Cooperative detection for mmwave radar-communication systems," in *2020 IEEE International Conference on Communications Workshops (ICC Workshops)*. IEEE, pp. 1–6, 2020.

[17] Zixi Fang, Zhiqing Wei, Zhiyong Feng, Xu Chen, and Zijun Guo, "Performance of joint radar and communication enabled cooperative detection," in *2019 IEEE/CIC International Conference on Communications in China (ICCC)*. IEEE, pp. 753–758, 2019.

[18] Xu Chen, Zhiqing Wei, Zixi Fang, Hao Ma, Zhiyong Feng, and Huici Wu, "Performance of joint radar-communication enabled cooperative uav network," in *2019 IEEE International Conference on Signal, Information and Data Processing (ICSIDP)*. IEEE, pp. 1–4 ,2019.

[19] Akram Al-Hourani, Robin J Evans, Sithamparanathan Kandeepan, Bill Moran, and Hamid Eltom, "Stochastic geometry methods for modeling automotive radar interference," *IEEE Transactions on Intelligent Transportation Systems*, vol. 19, no. 2, pp. 333–344, 2017.

[20] Sung Nok Chiu, Dietrich Stoyan, Wilfrid S Kendall, and Joseph Mecke, *Stochastic geometry and its applications*, John Wiley & Sons, 2013.

[21] Aymen Omri and Mazen O. Hasna, "Modeling and performance analysis of d2d communications with interference management in 3-d hetnets," in *2016 IEEE Global Communications Conference (GLOBECOM)*, 2016, pp. 1–7.